Single-crystalline $BiMnO_3$ studied by temperature-dependent x-ray diffraction and Raman spectroscopy

P. Toulemonde,[1,2,*] P. Bordet,[1,2] P. Bouvier,[3] and J. Kreisel[4,5]
[1]*Université Grenoble Alpes, Institut Néel, F-38042 Grenoble, France*
[2]*CNRS, Institut Néel, F-38042 Grenoble, France*
[3]*Laboratoire des Matériaux et du Génie Physique, CNRS, Grenoble Institute of Technology, 3 parvis Louis Néel, F-38016 Grenoble, France*
[4]*Département Science et Analyse des Matériaux, CRP Gabriel Lippmann, 41 rue du Brill, L-4422 Luxembourg*
[5]*Physics and Materials Science Research Unit, University of Luxembourg, 41 Rue du Brill, L-4422 Belvaux, Luxembourg*
(Received 4 April 2014; revised manuscript received 10 June 2014; published 30 June 2014)

We report on the temperature dependence of the phonons and crystallographic parameters in $BiMnO_3$ single crystals grown under high pressure and high temperature. The crystallographic structure of the sample was refined from room temperature to liquid helium temperature in the centrosymmetric $C2/c$ space group, i.e., a group which does not allow ferroelectricity. In addition, the lattice dynamics was probed by Raman spectroscopy down to liquid nitrogen temperature, i.e., below the ferromagnetic transition at $T_C = 100 \pm 2$ K. Both crystallographic and Raman data indicate the absence of a structural phase transition at the ferromagnetic ordering or any other temperature. The Raman signature around T_C shows a significant spin-phonon coupling for the high-frequency bands.

DOI: 10.1103/PhysRevB.89.224107 PACS number(s): 75.85.+t, 74.25.nd, 78.30.−j, 61.05.cp

I. INTRODUCTION

Bismuth-based BiMO$_3$ oxides with M being a 3d transition metal or a IIIA element (Al, Ga, In) crystallize in a distorted perovskite crystal structure. The effect of the $6s^2$ lone pair electrons of bismuth dominates the distortion of the ideal cubic perovskite. Depending on the 3d element, Bi-based perovskites exhibit various physical properties (for a review with M different from Fe, see Ref. [1]), including multiferroism when M = Fe (for a review on $BiFeO_3$, see Ref. [2]). Because of the Bi^{3+} off-centering induced by stereochemically active $6s^2$ lone pairs, the majority of theses oxides can only be prepared by high pressure–high temperature (HP-HT) synthesis in their bulk form (or in thin films), namely, for isostructural BiMO$_3$ with M = Sc, Mn, and Cr 3d transition metals. While $BiScO_3$ is nonmagnetic [3,4], $BiCrO_3$ is a canted antiferromagnet below $T_N = 109$ K [5,6] and bismuth manganite, $BiMnO_3$ (BMO), is ferromagnetic (FM) below $T_C = 99$–103 K [6].

BMO is still a controversial material. More than 10 years ago it was presented as a multiferroic system, i.e., a ferroelectric and ferromagnetic material at low temperature, based on electrical polarization hysteresis loops measured on bulk polycrystalline samples [7]. In addition, in the first crystallographic studies of BMO, the structure was refined in a noncentrosymmetric space group, $C2$, which allows ferroelectricity [8]. Nevertheless, the reported nonsaturation of the polarization loops and the fact that this measurement was not reproduced in bulk samples makes one question its ferroelectric nature. Several more recent studies based on electron and neutron diffraction [9,10] on polycrystalline samples have put into question the $C2$ initial choice and have pointed towards a centrosymmetric space group, $C2/c$, which excludes ferroelectricity.

Recently, following the work of Azuma *et al.* [11], we have grown small BMO single crystals (with a typical size of 20–100 μm long). Such single crystals, not embedded with secondary phases such as Bi_2O_3 that we found in polycrystalline samples, provide a strong signal in Raman spectroscopy and allow a more precise crystallographic investigation, compared to powder studies. We have characterized them at room temperature (RT), in particular, by x-ray diffraction (XRD) and Raman spectroscopy, which confirm that BMO adopts the nonpolar $C2/c$ space group at ambient conditions [12]. In our recent high pressure investigation of BMO up to 60 GPa we have observed multiple phase transitions, thus instabilities, namely, an intriguing and unexpected phase which allows ferroelectricity [13].

The aim of the present paper is to investigate the low temperature regime of BMO single crystals. For this, we have studied both the crystallographic structure and the phonons in the 4–300 K range. We have found that BMO remains in its initial centrosymmetric structure down to 4 K and that the two highest phonon modes show anomalies close to the ferromagnetic transition that we interpret as spin-lattice coupling.

II. EXPERIMENT

The BMO single crystals were obtained at HP-HT using boron hydroxide as the flux in a belt-type apparatus, as described previously [12]. The sample was checked by laboratory x-ray powder diffraction ($\lambda_{Cu,K\alpha_{1,2}} = 1.5418$ Å). Then, the flux was dissolved and the BMO single crystals were selected (among other Mn_3O_4 crystals which form as a secondary phase) by Raman spectroscopy using their established Raman signature (see Fig. 2 in our previous work [12]). Magnetization measurements were performed with a Quantum Design superconducting quantum interference device (SQUID) magnetometer between RT and 2 K and with a magnetic field up to 5 T (resolution: 2×10^{-11} A m^2).

*Corresponding author: pierre.toulemonde@neel.cnrs.fr

A BMO single crystal of irregular shape with 0.1 mm maximum dimension was selected for the x-ray diffraction experiment. A Bruker AXS Kappa APEX-II diffractometer equipped with graphite monochromatized Ag$K\alpha$ radiation ($\lambda = 0.56087$ Å) was used. After unit cell and orientation matrix determination, diffraction data were recorded using a series of phi and omega scans with a 0.5° frame width, leading to a redundancy of 6 in the $2/m$ point group up to $\theta = 34°$ ($\sin\theta/\lambda = 0.997$). No sign of twinning could be detected by inspection of the diffraction images. The low temperature measurements were carried out with the same instrument, using a fixed helium bath cryostat containing a sample orientation device magnetically coupled to the diffractometer [14]. Data collections were carried out at 150, 90, 60, 25, and 4.8 K with a temperature stability of 0.1 K. Two 360° phi scans separated by a 70° omega scan were measured at $\theta = 15°$ and $\kappa = 54°$ imposed by the geometry of the small two-axes goniometric device enclosed in the cryostat. The integrated intensities were extracted with the EVALCCD software [15]. An anisotropic absorption correction was applied using SADABS [16] assuming a $2/m$ point group, followed by a spherical absorption correction ($R = 0.05$ mm, $\mu = 30.854$ mm^{-1}). The refinements were carried out using the JANA2006 software [17].

Raman spectra versus temperature were registered using a Jobin-Yvon Labram spectrometer equipped with a single notch filtering and liquid nitrogen cooled CCD detector. The measurements were performed without heating or damaging the sample using an adapted power of the excitation laser with a wavelength of 632.8 nm. The BMO single crystal was placed in a commercial cell (Linkam) cooled by liquid nitrogen flux and regulated in temperature with an internal resistive heater.

III. RESULTS AND DISCUSSION

Figure 1 displays the magnetization curve of a typical BMO single crystal (around 1 μg) measured at 100 Oe as a function of temperature and examples of isothermal magnetization measured at 2, 150, and 300 K. At RT the crystal is paramagnetic while below $T_C = 100 \pm 2$ K it becomes ferromagnetic, consistent with previous reports [7,18]. In the following we have investigated such single crystals by XRD and Raman spectroscopy.

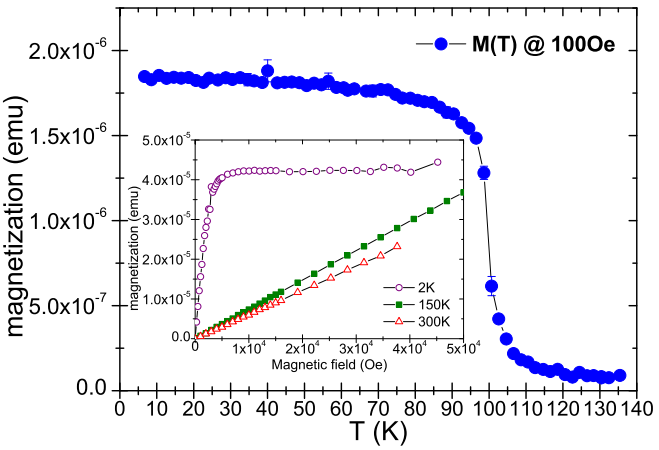

FIG. 1. (Color online) Temperature dependence of the magnetization measured at 100 Oe on a $BiMO_3$ single crystal. Inset: Isothermal magnetization of the same crystal as a function of magnetic field at $T = 2$, 150, and 300 K.

A. Crystallographic structure versus temperature

Here the crystallographic parameters of BMO are investigated as a function of temperature on single crystals. Figure 2 shows a representative reconstruction of one of the reciprocal planes. No reflections with $I > 5\sigma(I)$ were found to break the C centering or the c glide mirror extinction rule, as confirmed by reconstructed images of the ($h0l$) reciprocal planes observed at 300 and 4.8 K (Fig. 2). The refinements were carried out in the $C2/c$ space group symmetry, starting from the values reported by Montanari *et al.* [10]. Attempts to refine in the noncentrosymmetric $C2$ space group proposed by Atou *et al.* [8], including the possibility of merohedral twinning, lead to poorer agreement factors and difficult convergence due to correlations between parameters.

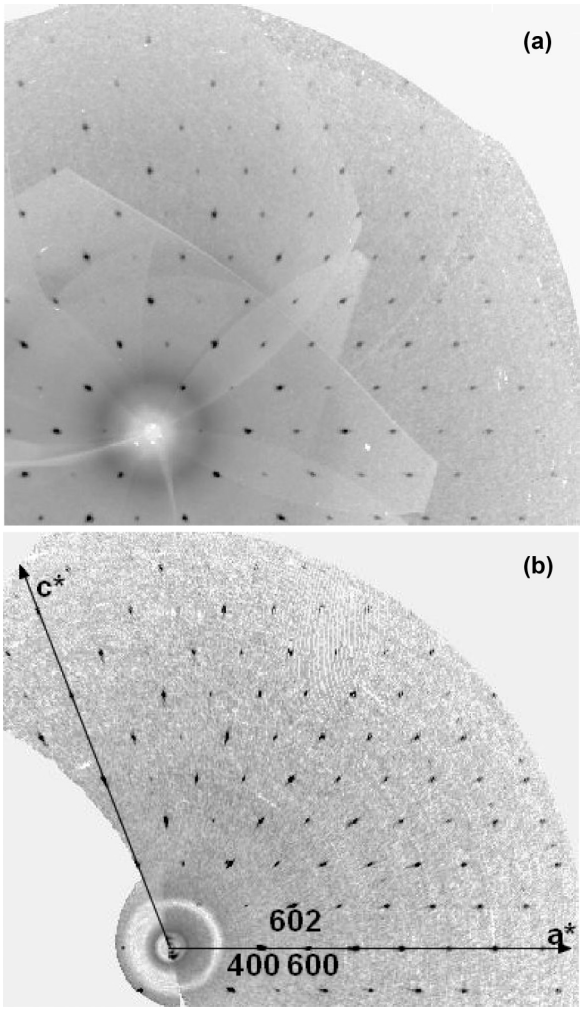

FIG. 2. Reconstruction of the $BiMnO_3$ ($h0l$) plane obtained from single-crystal x-ray diffraction at $\lambda_{Ag,K\alpha_1} = 0.56087$ Å at (a) $T = 300$ K and (b) 4.8 K showing the absence of reflections with h or l odd, consistent with a $C2/c$ symmetry.

TABLE I. Lattice, positional, and atomic displacement parameters for a $BiMnO_3$ single crystal at 4.8 K (first row) and 300 K (second row), from single-crystal x-ray diffraction data refined in the $C2/c$ space group ($\lambda_{Ag,K\alpha 1} = 0.5608$ Å).

T (K)		a (Å)	b (Å)	c (Å)	β (deg)
4.8		9.569(1)	5.602(1)	9.879(1)	111.02(1)
300		9.552(1)	5.627(1)	9.878(1)	110.70(1)
Atom	Wyckoff site	x	y	z	U_{iso} (Å^2) $\times 10^3$
Bi	8f	0.13656(4)	−0.21734(9)	0.12697(4)	4.77(12)
		0.13663(4)	−0.21890(7)	0.12656(4)	7.45(10)
Mn1	4e	0	0.2113(6)	0.25	5.8(6)
		0	0.2106(4)	0.25	5.5(5)
Mn2	4c	0.25	0.25	0	3.5(6)
		0.25	0.25	0	4.0(5)
O1	8f	0.0991(11)	0.1776(19)	0.0815(10)	8(3)
		0.0993(8)	0.1724(15)	0.0822(9)	9(2)
O2	8f	0.3524(10)	0.4567(18)	0.1646(9)	7(2)
		0.3537(8)	0.4519(14)	0.1635(8)	8.9(19)
O3	8f	0.1443(10)	0.434(2)	0.3639(9)	7(2)
		0.1444(8)	0.4283(17)	0.3660(9)	14(2)
T (K)	n_{obs}	n_{par}	R_{obs}	wR_{obs}	gof
4.8	1430	49	6.1	7.3	2.16
300	2054	49	5.5	6.8	2.28

The lattice parameters, and positional and atomic displacement parameters obtained after final convergence at 300 and 4.8 K, are displayed in Table I, and the evolution of the β angle of the monoclinic lattice and Mn-O bond lengths (around both Mn1 and Mn2 sites) versus temperature are shown in Fig. 3. Within the precision of our experiment, no anomaly could be detected on the thermal variation of the lattice parameters in the whole temperature range (not shown), including around the magnetic transition. This is consistent with the powder XRD data of Kimura *et al.* [18] and neutron powder diffraction studies of both Moreira *et al.* [19] and more recently of Chen *et al.* [20], who noticed no anomaly at T_C. On the other hand, also based on neutron powder diffraction data, Montanari *et al.* [10] reported anomalous changes in the relative variation of the a-axis parameter (below -0.5×10^{-3}) and the absolute value of the β angle (around -0.06°) proportional to the square of the ordered magnetic moment of Mn at T_C related to large magnetoelastic effects. In the present single-crystal study we are only sensitive to the slight decrease of the β angle (with a similar change around -0.1°) at T_C [Fig. 3(a)]. As mentioned before, considering the incertitude of our refined crystallographic data, no anomaly on the Mn-O bond lengths variation can be observed [Figs. 3(b) and 3(c)], in particular, around T_C; in addition, we note that the cooperative Jahn-Teller distortion measured at RT does not evolve significantly with temperature, remaining around 14.7% and 13% at the Mn2 and Mn1 sites, respectively.

B. Phonons modes versus temperature

In order to further analyze structural changes with temperature, we have investigated BMO by using Raman spectroscopy, which is known as a sensitive technique for detecting phase transitions or more subtle structural rearrangements due to coupling phenomena in ABO_3 perovskites [21,22]. Figure 4 presents representative unpolarized Raman spectra measured on a BMO single crystal in the range of 78–325 K. The room temperature spectrum is identical to our earlier reported signature [12] (confirmed by Goian *et al.* [23]). Sixteen phonon modes are observed in the 50–800 cm^{-1} range, which is compatible with the 27 modes expected in the case of the $C2/c$ description of the crystal obtained from XRD (while 60 modes would be Raman active in the noncentrosymmetric $C2$ space group). With decreasing temperature we observe, as expected, a high-frequency shift and significant sharpening of all bands, which is well understood by considering thermal contraction and the reduction of thermal vibrations, respectively. Apart from such thermal effects, the overall spectral signature is maintained throughout the whole temperature, which strongly suggests the absence of a phase transition. Figure 5 displays the evolution of the different phonon modes with temperature, showing the absence of any significant anomalies in terms of change in wave number (see also Table II), or additional or suppressed bands, again supporting the absence of a structural phase transition in the investigated temperature range. However, on the basis of literature work on improper ferroelectric manganites [24], we cannot entirely rule out the associated very subtle structural rearrangement which would be below the detection limit of the XRD and Raman probes described here.

Having said that, it is now interesting to note that a closer look at the high-frequency bands ($\nu_1 \approx 636$ cm^{-1} and $\nu_2 \approx 530$ cm^{-1} at RT) shows a slight but distinctive departure from the frequency evolution expected from the Grüneisen temperature behavior, shown as a dotted line in Fig. 6 (fitted by $\omega_j = \omega_{j0}\{1 - c_j/[\exp(\theta_D/T) - 1]\}$ with the Debye temperature $\theta_D = 410$ K taken from Ref. [4]). Such slight changes are usually understood within the concept of hard mode spectroscopy [25,26] and indicate subtle structural rearrangements due to changes in the local lattice coupling. Both high-frequency bands show a sudden anomaly and a low-frequency shift around 100–110 K, so it is right in

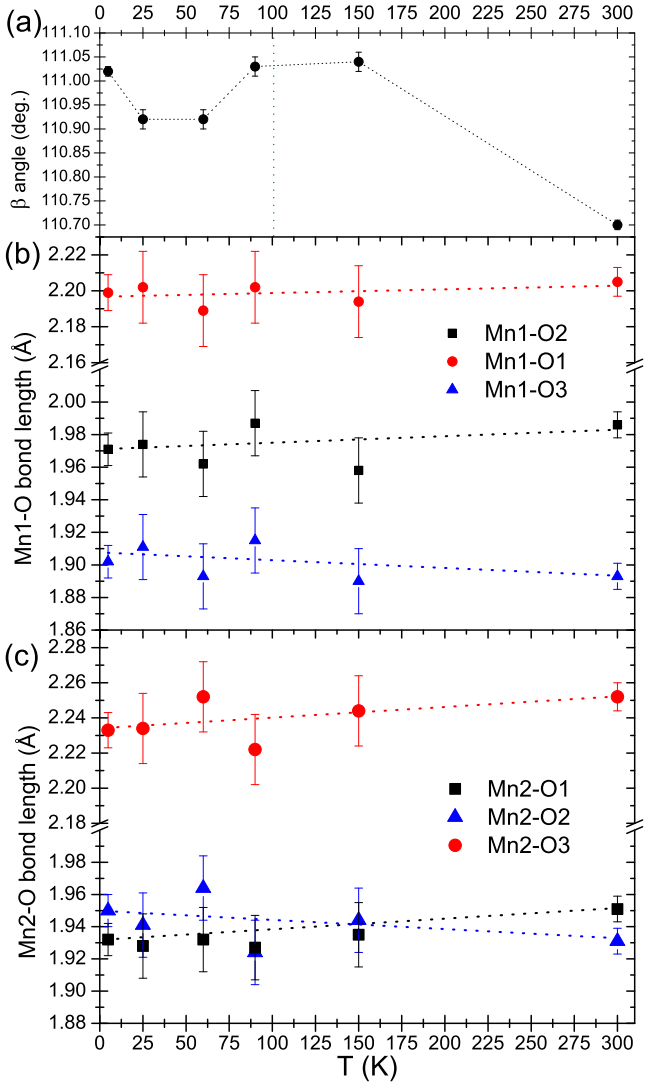

FIG. 3. (Color online) Temperature dependence of the refined (a) β angle, (b) Mn1-O, and (c) Mn2-O bond lengths in the $BiMnO_3$ single crystal described in its $C2/c$ monoclinic lattice.

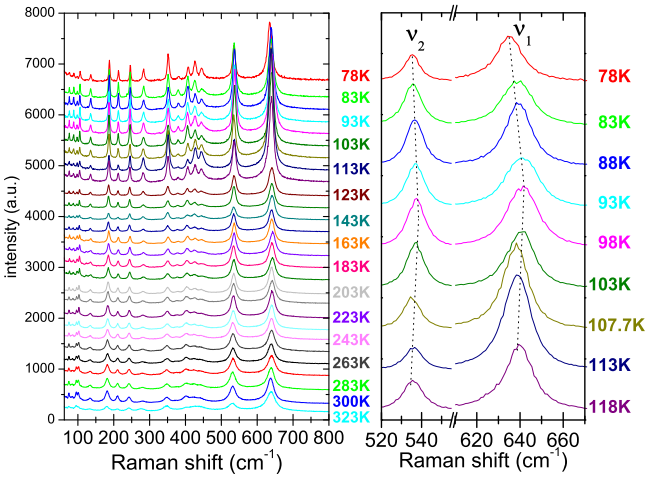

FIG. 4. (Color online) Left: Raman spectra of a $BiMnO_3$ single crystal recorded between 325 K (bottom) and 78 K (top). Right: High-frequency range with ν_1 and ν_2 bands.

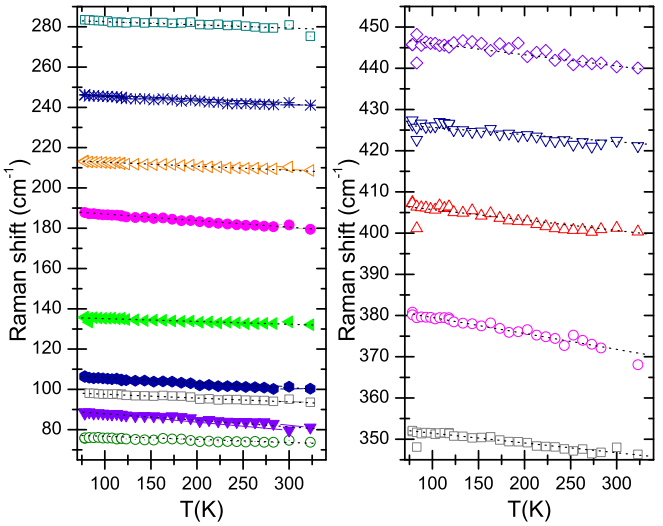

FIG. 5. (Color online) Temperature dependence of the $BiMnO_3$ Raman-active phonon modes in the 60–470 cm^{-1} range.

the range of the ferromagnetic phase transition presented in Sec. III A. As a consequence, it is natural to attribute this anomaly to a spin-phonon coupling when entering the low temperature ferromagnetic phase from the high temperature paramagnetic phase. The type and strength of the observed anomaly is reminiscent of earlier reported Raman signatures of spin-phonon coupling in $AMnO_3$ perovskites [22,27]. Generally speaking, the frequency shift of a given phonon as a function of temperature, due to the spin-phonon coupling, is determined by the spin-spin correlation function [28,29]. In the presence of competing ferromagnetic and antiferromagnetic (AFM) interactions, it was proposed that the frequency shift

TABLE II. Positions in wave number (at 300 K) and slope values of the linear curve fits (in the 78–320 K range) drawn in Fig. 5 for each Raman mode of a $BiMnO_3$ single crystal.

ω (cm^{-1}) at 300 K	$d\omega/dT$ (cm^{-1}/K) $\times 10^2$
75.0(5)	−1.01(1)
83.7(5)	−2.98(2)
95.5(5)	−1.86(1)
100.8(5)	−2.57(1)
133.6(5)	−1.32(1)
181.6(5)	−3.22(1)
210.3(5)	−1.66(1)
242.3(5)	−2.13(1)
280.3(5)	−1.93(2)
348.0(5)	−2.23(2)
371.9(5)	−4.06(2)
401.5(5)	−2.84(3)
424.1(5)	−2.28(2)
441.2(5)	−2.38(3)
531.8(5)	−2.92(2)[a]
637.4(5)	−1.78(4)[a]

[a]Linear fit above 105 K.

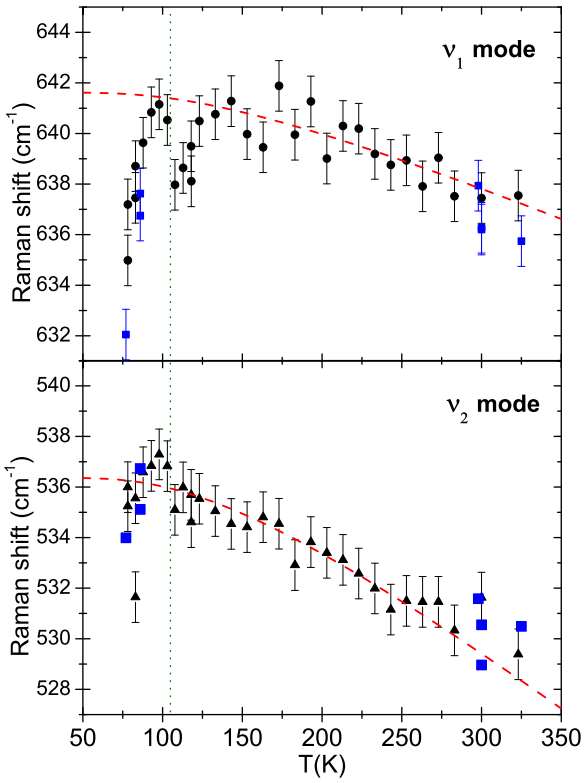

FIG. 6. (Color online) Temperature dependence of the $BiMnO_3$ Raman-active phonon modes in the 470–650 cm^{-1} range (from two experiments). Dotted line (red): Comparison with a temperature dependence given by the model $\omega_j = \omega_{j0}\{1 - c_j/[\exp(\theta_D/T) - 1]\}$.

can be described by [28,30]

$$\omega - \omega_0 \propto -R_1\langle \vec{S_i} \mid \vec{S_j}\rangle + R_2\langle \vec{S_i} \mid \vec{S_k}\rangle,$$

where R_1 and R_2 are spin-dependent force constants of the lattice vibrations deduced from the exchange integrals with the respect to the phonon displacement. R_1 is associated with the ferromagnetic nearest neighbor and R_2 is associated with the antiferromagnetic next nearest neighbor exchange. As a consequence, the upward or downward shift of a phonon at the magnetic phase transitions derives from the presence of FM and AFM interactions, which can lead in perovskite-type $AMnO_3$ solid solutions to either trends, depending on the chemical composition [31]. In our present case of BMO, the two high-frequency bands are dominated by breathinglike vibrations of the light oxygens in the MnO_6 octahedra (see also the recent assignment of Raman modes of BMO in the $C2/c$ space group by Kozlenko *et al.* [32]) and the downward shift of their frequencies indicate that they are dominated by FM intercations. We note that the above-discussed anomalies were not observed in the infrared study of polycrystalline BMO, which have been recently studied as a function of temperature by Goian *et al.* [23], which is likely due to the limited number of only five investigated temperatures, probably insufficient for detecting subtle changes. Finally, we should point out that the two modes discussed here are not the soft modes at 72.4 and 98.2 cm^{-1} for which Hill and Rabe predicted in their original calculations an unstable behavior at the origin of ferroelectricity and ferromagnetism in BMO [33].

IV. CONCLUSION

We have studied single crystals of $BiMnO_3$ grown at HP-HT from RT to low temperature by means of magnetometry, x-ray diffraction, and Raman scattering. We found that the refined crystallographic structure solved on a single crystal of $BiMnO_3$ is centrosymmetric and belongs to the $C2/c$ space group, i.e., a group which does not allow ferroelectricity. At low temperature the crystal remains in this symmetry and does not show a crystallographic phase transition at the ferromagnetic transition at $T_C = 100 \pm 2$ K, as evidenced by magnetization measurements. This is corroborated by studying the lattice dynamics using Raman spectroscopy down to 77 K. At T_C we observe slight but distinct anomalies for the two high-frequency Raman bands, which we interpret as a spin-phonon coupling.

ACKNOWLEDGMENTS

The authors thank V. Simonet and E. Eyraud (Institut Néel, Grenoble) for their help with the magnetic measurements. J.K. acknowledges support from the National Research Fund, Luxembourg (FNR/P12/4853155).

[1] A. A. Belik, J. Solid State Chem. **195**, 32 (2012).
[2] G. Catalan and J. F. Scott, Adv. Mater. **21**, 2463 (2009).
[3] A. A. Belik, S. Iikubo, K. Kodama, N. Igawa, S. Shamoto, M. Maie, T. Nagai, Y. Matsui, S. Yu. Stefanovich, B. I. Lazoryak, and E. Takayama-Muromachi, J. Am. Chem. Soc. **128**, 706 (2006).
[4] A. A. Belik and E. Takayama-Muromachi, Inorg. Chem. **45**, 10224 (2006).
[5] C. Darie, C. Goujon, M. Bacia, H. Klein, P. Toulemonde, P. Bordet, and E. Suard, Solid State Sci. **12**, 660 (2010).
[6] F. Sugawara, S. Iiida, Y. Syono, and S. Akimoto, J. Phys. Soc. Jpn. **25**, 1553 (1968).
[7] A. Moreira dos Santos, S. Parashar, A. R. Raju, Y. S. Zhao, A. K. Cheetham, and C. N. R. Rao, Solid State Commun. **122**, 49 (2002).
[8] T. Atou, H. Chiba, K. Ohoyama, Y. Yamaguchi, and Y. Syono, J. Solid State Chem. **145**, 639 (1999).
[9] A. A. Belik, S. Iikubo, T. Yokosawa, K. Kodama, N. Igawa, S. Shamoto, M. Azuma, M. Takano, K. Kimoto, Y. Matsui, and E. Takayama-Muromachi, J. Am. Chem. Soc. **129**, 971 (2007).
[10] E. Montanari, G. Calestani, L. Righi, E. Gilioli, F. Bolzoni, K. S. Knight, and P. G. Radaelli, Phys. Rev. B **75**, 220101(R) (2007).
[11] M. Azuma, T. Saito, S. Ishiwata, I. Yamada, Y. Kohsaka, H. Takagi, and M. Takano, Physica C **392**, 22 (2003).

[12] P. Toulemonde, C. Darie, C. Goujon, M. Legendre, T. Mendonca, M. Alvarez-Murga, V. Simonet, P. Bordet, P. Bouvier, J. Kreisel, and M. Mezouar, High Pressure Res. **29**, 600 (2009).
[13] M. Guennou, P. Bouvier, P. Toulemonde, C. Darie, C. Goujon, P. Bordet, M. Hanfland, and J. Kreisel, Phys. Rev. Lett. **112**, 075501 (2014).
[14] P. Fertey, R. Argoud, P. Bordet, J. Reymann, C. Palin, C. Bouchard, R. Bruyère, E. Wenger, and C. Lecomte, J. Appl. Crystallogr. **40**, 526 (2007).
[15] A. J. M. Duisenberg, L. M. J. Kroon-Batenburg, and A. M. M. Schreurs, J. Appl. Crystallogr. **36**, 220 (2003).
[16] G. M. Sheldrick, SADABS, University of Göttingen, Germany, 1996.
[17] V. Petricek, M. Dusek, and L. Palatinus, JANA2006: The Crystallographic Computing System, Institute of Physics, Praha, Czech Republic, 2006.
[18] T. Kimura, S. Kawamoto, I. Yamada, M. Azuma, M. Takano, and Y. Tokura, Phys. Rev. B **67**, 180401(R) (2003).
[19] A. Moreira dos Santos, A. K. Cheetham, T. Atou, Y. Syono, Y. Yamaguchi, K. Ohoyama, H. Chiba, and C. N. R. Rao, Phys. Rev. B **66**, 064425 (2002).
[20] W.-T. Chen, F. Sher, N. D. Mathur, C. M. Kavanagh, F. D. Morrison, and J. P. Attfield, Chem. Mater. **24**, 199 (2012).
[21] M. Guennou, P. Bouvier, G. S. Chen, B. Dkhil, R. Haumont, G. Garbarino, and J. Kreisel, Phys. Rev. B **84**, 174107 (2011).
[22] J. Laverdière, S. Jandl, A. A. Mukhin, V. Y. Ivanov, V. G. Ivanov, and M. N. Iliev, Phys. Rev. B **73**, 214301 (2006).
[23] V. Goian, S. Kamba, M. Savinov, D. Nuzhnyy, F. Borodavka, P. Vanek, and A. A. Belik, J. Appl. Phys. **112**, 074112 (2012).
[24] H. C. Walker, F. Fabrizi, L. Paolasini, F. de Bergevin, J. Herrero-Martin, A. T. Boothroyd, D. Prabhakaran, and D. F. McMorrow, Science **333**, 1273 (2011).
[25] E. K. H. Salje and U. Bismayer, Phase Transitions **63**, 1 (1997).
[26] U. Bismayer, Phase Transitions **27**, 211 (1990).
[27] W. S. Ferreira, J. Agostinho Moreira, A. Almeida, M. R. Chaves, J. P. Araújo, J. B. Oliveira, J. M. Machado Da Silva, M. A. Sá, T. M. Mendonça, P. Simeão Carvalho, J. Kreisel, J. L. Ribeiro, L. G. Vieira, P. B. Tavares, and S. Mendonça, Phys. Rev. B **79**, 054303 (2009).
[28] W. Baltensperger and J. S. Helman, Helv. Phys. Acta **41**, 668 (1968).
[29] D. J. Lockwood and M. G. Cottam, J. Appl. Phys. **64**, 5876 (1988).
[30] K. Wakamura and T. Arai, J. Appl. Phys. **63**, 5824 (1988).
[31] J. Agostinho Moreira, A. Almeida, W. S. Ferreira, J. P. Araújo, A. M. Pereira, M. R. Chaves, M. M. R. Costa, V. A. Khomchenko, J. Kreisel, D. Chernyshov, S. M. F. Vilela, and P. B. Tavares, Phys. Rev. B **82**, 094418 (2010).
[32] D. P. Kozlenko, N. T. Dang, S. H. Jabarov, A. A. Belik, S. E. Kichanov, E. V. Lukin, C. Lathe, L. S. Dubrovinsky, V. Yu. Kazimirov, M. B. Smirnov, B. N. Savenko, A. I. Mammadovc, E. Takayama-Muromachi, and L. H. Khiem, J. Alloys Compd. **585**, 741 (2014).
[33] N. A. Hill and K. M. Rabe, Phys. Rev. B **59**, 8759 (1999).